DJ Journal of Engineering Chemistry and Fuel, Vol. 1(4) 2016, pp. 1-16

RESEARCH ARTICLE

Experimental and Quantum Chemical Studies on the Corrosion Inhibition of Mild Steel by Quinoline Schiff Bases

[*]P.M Dasami[1], K Parameswari[1], S Chitra[1], K Jayamoorthy[2]

[1]Department of Chemistry, PSGR Krishnammal College for Women, Peelamedu, Coimbatore-621004 Tamilnadu, India.

[2]Department of Chemistry, St.Joseph's College of Engineering, Chennai, 600119 Tamilnadu, India.

Received- 10 July 2016, Revised- 13 August 2016, Accepted- 1 September 2016, Published- 7 September 2016

ABSTRACT

The inhibiting effect of two synthesized quinolone Schiff bases(SB1& SB2) on mild steel corrosion in 1M H_2SO_4 was evaluated using weight loss and electrochemical measurements. The Schiff bases reduce the corrosion of mild steel. The efficiency was concentration and temperature dependent. Polarization studies indicated that the Schiff bases are mixed type inhibitors and they function by adsorption obeying Langmuir isotherm. Quantum chemical studies showed that the inhibition efficiency correlated well with the E_{HOMO}, energy gap and total energy. Fukui function analysis through DFT calculations were used to predict the possible centres for adsorption and inhibition.

Keywords: Corrosion inhibition, Schiff base, Electrochemical study, Synergism, Theoretical study.

1. INTRODUCTION

Mild steel corrosion is a major problem faced by many industries where acids are widely used for acid pickling, acid descaling and oil-well acidizing [1]. Corrosion inhibitors are needed to reduce the corrosion rates of metallic materials in acid media [2]. Most of the efficient inhibitors used in industry are organic compounds which mainly contain oxygen, sulphur, nitrogen atoms and multiple bonds in the molecule through which they are adsorbed on metal surface [3-6].

Quantum chemical studies are often used to elucidate the physical as well as chemical properties of organic compounds and to understand the corrosion inhibition mechanism [7-9]. Recently, density functional theory has proven to be an important tool to analyze the characteristics of the inhibitors/metal surface interactions and to elucidate the centres in the compounds on which such interactions are likely to occur [10-12]. Localization of frontier molecular orbitals (HOMO& LUMO) and condensed Fukui indices (f_k^+&f_k^-) analysis of the reactive regions are very useful in characterizing organic adsorbate.

Schiff bases have been used as effective corrosion inhibitors, which is based on their ability to spontaneously form a monolayer on the surface to be protected.

The aim of the present work is to carry out corrosion inhibition studies on two synthesized quinolone Schiff bases by experimental and quantum chemical studies and also to determine a relationship between the quantum chemical parameters obtained from their structure and the IE obtained experimentally.

2. EXPERIMENTAL

Structure of the Schiff bases is depicted in the schematic shown in figure B1.

2.1. FTIR Spectroscopy

Figure B2 shows the FTIR spectrum for SB1. The data is given below.

3172 cm^{-1} (O-H), 1608 cm^{-1} (C=N), 1518 cm^{-1} (C=C ring stretching), 704cm^{-1} (C-S)

*Corresponding author. Tel.: +919633020668

Email address: pmdasami@gmail.com (P.M.Dasami)

Double blind peer review under responsibility of DJ Publications

http://dx.doi.org/10.18831/djchem.org/2016041001

2.2. Materials used

The experiments were performed with cold rolled mild steel specimens of chemical composition (C=0.20%, Mn=1%, Si-0.05%, S=0.025%, P=0.25% and Fe=98%). Rectangular mild steel specimen of dimension 3cm x 1cm x 0.1cm were used for mass loss measurements. A cylindrical mild steel rod with an exposed area of 0.785cm^2 was used as the working electrode in electrochemical studies. The specimens were mechanically abraded with different grades of emery papers, degreased with acetone, washed and dried.

2.3. Instruments used

Mass loss experiments were performed with electrical weighing balance and Denver instrument. Electrochemical studies were carried out on IVIUM Compactstat (galvanostat/potentiostat) with a three electrode cell. Saturated Calomel Electrode (SCE) was used as reference electrode, platinum foil as the counter or auxiliary electrode and mild steel rod as the working electrode. The potential range was -200 to +200 mV with respect to the open circuit potential at a scan rate of 1mV/sec. For impedance measurements, the sweep frequency is from 10Hz to 0.01Hz with a signal amplitude of 10mV. The optimized molecular geometry of the compounds were performed using Gaussian 09 software with hybrid DFT functional (B3LYP/6-31+G(d,p)).

2.4. Measurements

The mild steel specimens were weighed before and after immersion in 1M H_2SO_4 containing various concentration of inhibitors for 3 hrs at various temperatures (303K-333K). Triplicate measurements were made and average mass loss was recorded. From the loss in mass, inhibition efficiency was calculated. Synergistic effect of the inhibitors was evaluated by the addition of halide ions in the inhibitor-acid solution. The inhibitor efficiency is given in equation (2.1)

$$\text{Inhibitor Efficiency (IE \%)} = \frac{\text{Weightloss}_{\text{blank}} - \text{Weightloss}_{\text{inhibitor}}}{\text{Weightloss}_{\text{blank}}} \text{ X } 100 \quad (2.1)$$

From the potentiodynamic polarization study, corrosion current density (I_{corr}), Tafel slopes [anodic (ba) and cathodic (bc)] and corrosion potential (E_{corr}) were calculated. Inhibition efficiency was obtained from the corrosion current density (I_{corr}) as shown in equation (2.2)

$$\text{Inhibitor Efficiency (\%)} = \frac{I_{corr(blank)} - I_{corr(inh)}}{I_{corr(blank)}} \text{ X } 100 \quad (2.2)$$

Double layer capacitance (Cdl) and charge transfer resistance(Rct) values were obtained from AC impedance spectroscopy. Inhibition efficiency was calculated from Rct value as in equation (2.3)

$$\text{Inhibitor Efficiency (\%)} = \frac{R_{ct(inh)} - R_{ct(blank)}}{R_{ct(inh)}} \text{ X } 100 \quad (2.3)$$

The quantum chemical parameters E_{HOMO}, E_{LUMO}, energy gap (ΔE) and other parameters, including electronegativity (χ), global hardness (Π), global softness (S), dipole moment, chemical potential, electrophilicity, ionization potential (I), electron affinity (A) and the fraction of electrons transferred from the inhibitor molecule to the metallic atom (ΔN) were calculated. The local reactivity was analyzed through Fukui function, which is calculated from the Mulliken charges.

For reaction with the electrophiles:

$$f_k^- = qN - qN\text{-}1$$

For reaction with the nucleophiles:

$$f_k^+ = qN + 1 - qN$$

3. RESULTS AND DISCUSSIONS

3.1. Weight loss measurements

The inhibition efficiencies attained from mass loss studies of mild steel at different inhibitor concentrations and at various intervals of immersion were tabulated in table A1. As inhibitor concentration increased IE also increased.. The maximum inhibition efficiency was observed at 0.5mM inhibitor concentration. Beyond this, the IE remained almost constant. As time increases the adsorption of the inhibitor molecule also increased and reached a maximum at 3hrs of immersion. After that, the IE value decreased drastically. Hence, it can be concluded that the inhibitor is active upto 3 hrs in acid medium. The corrosion rate and IE obtained from mass loss data at higher temperatures (303K-333K) as given in table A2 showed that the inhibitors are effective even at 333K displaying > 90'%

efficiency. The decrease in efficiency at longer duration may be due to desorption of the inhibitors.

Synergistic effect was studied by adding halide ions to the acid-inhibitor solution. The results in table A3 showed that the efficiency increased with the addition of halide ions and the synergism order is $Cl^-<Br^-<I^-$. Iodide ions showed higher efficiency because I- ions are strongly chemisorbed and form iron iodide. The chemisorption shifts ϕ_n of the metal to more positive potential and the metal surface becomes more negatively charged. Hence due to electrostatic interaction Protonated cationic inhibitor molecules are easily physisorbed .

3.2. Potentiodynamic polarization study

Figure B3 shows the potentiokintic polarization curve of mild steel immersed in 1M H_2SO_4 with selected concentrations of SB 2. Electrochemical corrosion parameters such as corrosion potential (E_{corr}), corrosion current **(**I_{corr}), inhibition efficiency and Tafel slopes (b_a & b_c) were found out and summarized in table A4. It is obvious that with the addition of the Schiff bases current density (I_{corr}) decreased. At the same concentration of 0.5mM, the Icorr value of steel with SB 2 is much smaller than that with SB 1 in 1M H_2SO_4. This enhanced efficiency is due to the presence of –SH group. E_{corr} values are marginally moved to the negative direction. The values of both b_a and b_c are changed owing to the addition of Schiff bases. This result advocates that the inhibitors are of mixed type [7].

3.3. Electrochemical impedance spectroscopic study

The corrosion response of mild steel in $1MH_2SO_4$ with and without inhibitor has been examined by impedance studies. The Nyquist plots obtained were analyzed by fitting to the equivalent circuit model (Figure B4 and figure B5) to describe the iron-acid interface [13]. The impedance parameters such as double layer capacitance (Cdl), charge transfer resistance (Rct) and Inhibition Efficiency (IE) derived from the model are listed in table A5. When the inhibitor concentration is increased, the Cdl values decreased and Rct increased. These results can be credited to the inhibitor adsorption at the metal solution interface to form a protective layer, which prevent mild steel dissolution [14]. It is clear that the Rct value increased to a maximum of 48.6 ohm/cm^2. In the case of SB 2, the effectiveness was indicated at 0.5mM concentration.

3.4. Adsorption isotherm and thermodynamic parameters

The mechanism of adsorption process is described by adsorption isotherms. The frequently used ones are Frumkin, Tempkin, Freudlich and Langmuir. The surface coverage degree (θ) for different Schiff bases concentrations were fitted to various isotherms. The best fit was shown by Langmuir isotherm (Figure B8) and is expressed as shown in (3.1).

$$\frac{Cinh}{\theta} = \frac{1}{K_{ads}} + Cinh \qquad (3.1)$$

where, C represents the inhibitor concentration, θ represents the fractional surface coverage, K_{ads} refers to the adsorption equilibrium constant and c is a constant.

Thermodynamic parameters were deducted from the Arrhenius plot (Figure B6) and transition state plot (Figure B7). The adsorption equilibrium constant, K got from the Langmuir adsorption isotherm is related to the standard free energy of adsorption ($\Delta G°_{ads}$) as shown in (3.2) [15]:

$$\Delta G^0_{ads} = -2.303RTlog(55.5K_{ads}) \qquad (3.2)$$

where, R refers to the universal gas constant, T represents the temperature and 55.5 is the molar concentration of water in the solution. Change in entropy (ΔS°) and enthalpy were obtained from transition state plot (Figure B6). The thermodynamic parameters are recorded in table A6.

The negative sign of $\Delta G_{ads}{}^0$ denotes that the inhibitor adsorption on the mild steel surface is a spontaneous process. The values are found to be less than -20KJ/mole which confirmed the physical adsorption [16]. Activation energy Ea in the presence of the inhibitors are higher than those in the free acid solution suggesting physical adsorption of inhibitors on metal surface. The negative signs of activation enthalpies (ΔH^0) reveal the exothermic nature of dissolution process. The negative value of entropies (ΔS^0) indicates that the activated complex in the rate determining step corresponds to association than dissociation process [17].

3.5. Quantum chemical study

Molecular orbital energies (E_{HOMO} and E_{LUMO}) are very important parameters used to predict the most reactive positions in Π-electron systems. The energy corresponding to HOMO is directly linked to the ionization potential and in the same way the LUMO energy is in direct relation with electron affinity. Larger E_{HOMO} values indicate higher tendency towards electron donation, increasing the inhibitor adsorption on mild steel surface and improved inhibition efficiency. E_{LUMO} represents the molecule's ability to accept electrons. With the increase in HOMO energy and decrease in LUMO energy, the binding ability of the inhibitor to the metal surface increases [18] (Figure B9 and figure B10). Lower energy gap values ($\Delta E=E_{LUMO}-E_{HOMO}$) result in good inhibition efficiencies, as the energy required to eliminate an electron from the last occupied orbital will be low. The ΔE of a molecule is a measure of the softness or hardness of a molecule. Hard molecules are characterized by larger values of ΔE and vice versa [7]. Comparing of the two Schiff bases revealed that SB 2 has lower ΔE value and hence possessed greater efficiency.

Dipole moment can be defined as a measure of polarity of a polar covalent bond. It can also be represented as the product of charge on the atoms and the distance between the two bonded atoms. However the global polarity of a molecule is evident from the total dipole moment [19]. No definite correlation has been reported in the literature for dipole moment and inhibition efficiency.

The number of transferred electrons (ΔN) was calculated and included in table A7. Δ*N* values showed that the inhibition efficiency resulting from electron donation is in close agreement with Lukovits's study. The inhibition efficiency increases with the electron-donating capability of the inhibitor. The outcomes show that Δ*N* values correlate strongly with experimental inhibition efficiencies. Thus, the highest electrons transfer fraction is associated with the better inhibitor (SB 2), while the least fraction is associated with the inhibitor that has the least inhibition efficiency (SB 1) [18].

The total energy of a molecule determines the reactivity and stability of a molecule. The higher the total energy (TE), higher is the stability of the molecule and lesser its tendency to donating electrons. The total energy of SB 1 is higher than SB 2 confirming higher IE of SB 2[7]

3.6. Mulliken charges and Fukui functions

Local softness indices and Fukui functions for nucleophilic and electrophilic attacks in inhibitor atoms can be calculated from Mulliken atomic charges. Table A8 and table A9 represents the neutral species (N) as well as the calculated Fukui indices (N+ 1 and N−1) for all the charged species of the Schiff bases. Condensed Fukui function helps in analyzing the local reactivity. The nucleophilic attack site will be the place where the $f+_k$ value is maximum and the electrophilic attack site is controlled by the $f-_k$ value [20].

3.7. Reason for the higher efficiency of SB 2 than SB 1

The average Fukui functions f_k^+ and f_k^- and the average local softness indices s_k + and s_k – of the four hetero atoms are calculated for the two Schiff bases in order to compare the efficiencies and the values are tabulated (table A10).

It is evident that f_k^+ and s_k+ values are higher for SB 2 indicating that SB 2 is more reactive than SB 1 in nucleophilic reaction with the iron surface [21, 22, 23]. Similarly, SB 2 is soft and hence react readily with soft Fe^{2+} ions on the mild steel surface.

4. CONCLUSIONS

- Two Schiff bases were prepared and their corrosion inhibition studies performance was evaluated.
- Weight loss studies showed that IE increases with increasing concentration and decreases with temperature.
- Electrochemical studies showed that both the inhibitors are mixed type in nature. The values observed were well correlated with the theoretical values.
- Both the theoretical and experimental data showed that the sulphur contained Schiff base have higher efficiency.
- Fukui functions for the Schiff bases were calculated by the Mulliken charges and thereby the electrophilic and nucleophilic attacking site was found out.

REFERENCES

[1] Mahdi Heydari, Fatemeh Baghaei Ravari and Athareh Dadgarineghad, Corrosion Inhibition Propargyl Alcohol on Low Alloy Cr Steel in 0.5 M H_2SO_4 in the Absence and Presence of Potassium Iodide, Gazi University Journal of Science, Vol. 24, No. 3, 2011, pp. 507-515.

[2] Ashish Kumar Singh, Sudhish Kumar Shukla and M.A.Quraishi, Corrosion Behaviour of Mild Steel in Sulphuric Acid Solution in Presence of Ceftazidime, International Journal of Electrochemical Science, Vol. 6, 2011, pp. 5802-5814.

[3] A.K.Singh, M.A.Quraishi, Adsorption Properties and Inhibition of Mild Steel Corrosion in Hydrochloric Acid Solution by Ceftobiprole, Journal of Applied Electrochemistry, Vol. 41, No. 1, 2011, pp. 7-18, http://dx.doi.org/10.1007/s10800-010-0202-y.

[4] P.Saravanan, K.Jayamoorthy, and S.Ananda Kumar, Design and Characterization of Non-Toxic Nano-Hybrid Coatings for Corrosion and Fouling Resistance, Journal of Science: Advanced Materials and Devices, 2016, http://dx.doi.org/10.1016/j.jsamd.2016.07.001

[5] S.Suresh, P.Saravanan, K.Jayamoorthy, S. Ananda Kumar and S.Karthikeyan, Development of Silane Grafted Zno Core Shell Nanoparticles Loaded Diglycidyl Epoxy Nanocomposites Film for Antimicrobial Applications, Materials Science and Engineering:C, Vol. 64, 2016 , pp. 286-292, http://dx.doi.org/10.1016/j.msec.2016.03.096.

[6] A.K.Singh and M.A.Quraishi, Investigation of Adsorption of Isoniazid Derivatives at Mild Steel/Hydrochloric Acid Interface: Electrochemical and Weight Loss Methods, Materials Chemistry and Physics,Vol. 123, No. 2-3, 2010 pp. 666-677, http://dx.doi.org/10.1016/j.matchemphys.2010.05.035.

[7] Ahmed M. Al-Sabagh, M. Notaila M.Nasser, Ahmed A.Farag, Mohamed A.Migahed, Abdelmonem M.F. Eissa and Tahany Mahmoud, Structure Effect of Some Amine Derivatives on Corrosion Inhibition Efficiency for Carbon Steel in Acidic Media using Electrochemical and Quantum Theory Methods, Egyptian Journal of Petroleum, Vol. 22, No. 1, 2013, pp. 101-116, http://dx.doi.org/10.1016/j.ejpe.2012.09.004.

[8] P.Udhayakala and T.V.Rajendran, A Theoretical Evaluation on Benzothiazole Derivatives as Corrosion Inhibitors on Mild Steel, Der Pharma Chemica, Vol. 7, No. 1, 2015, pp. 92-99.

[9] K.F.Khaled, Studies of Iron Corrosion Inhibition using Chemical, Electrochemical and Computer Stimulation Techniques, Electrochimica Acta, Vol. 55, No. 22, 2010, pp. 6523-6532, http://dx.doi.org/10.1016/j.electacta.2010.06.027.

[10] Nuha Ahmed Wazzan and Fatma Mohamed Mahgoub, DFT Calculations for Corrosion Inhibition of Ferrous Alloys by Pyrazolopyrimidine Derivatives, Open Journal of Physical Chemistry, Vol. 4, No. 1, 2014, pp. 6-14, http://dx.doi.org/10.4236/ojpc.2014.41002.

[11] Nnabuk O. Eddy, H. Momoh-yahaya and Emeka. E. Oguzie, Theoretical and Experimental Studies on the Corrosion Inhibition Potentials of Some Purines for Aluminium in 0.1M Hcl, Journal of Advanced Research, Vol. 6, No.2, 2015, pp. 203-217, http://dx.doi.org/10.1016/j.jare.2014.01.004.

[12] P.Udhayakala, A.Maxwell Samuel, T.V.Rajendran and

S.Gunasekaran, DFT Study on the Adsorption Mechanism of Some Phenyl Tetrazole Substituted Compounds as Effective Corrosion Inhibitors for Mild Steel, Der Pharma Chemica, Vol. 5, No. 6, 2013, pp. 111-124.

[13] E.E.Oguzie, Influence of Halide Ions on the Inhibitive Effect of Congo Red Dye on the Corrosion of Mild Steel in Sulphuric Acid Solution, Materials Chemistry and Physics, Vol. 87, No. 1, 2004, pp. 212-217, http://dx.doi.org/10.1016/j.matchemphys.2004.06.006.

[14] Amarish Singh, Ashish Kumar Singh and M.A.Quraishi, Dapsone: Anovel Corrosion Inhibitor for Mild Steel in Acid Media, The Open Electrochemistry Journal, Vol. 2, 2010, pp. 43-51.

[15] X.Joseph Raj and N. Rajendran, Corrosion Inhibition Effect of Substituted Thiadiazoles on Brass, International Journal of Electrochemical Science, Vol. 6, 2011, pp. 348 – 366.

[16] Taleb H.Ibrahim and Mohamed AbouZour, Corrosion Inhibition Of Mild Steel using Fig Leaves Extract in Hydrochloric acid Solution,International Journal of Electrochemical Science, Vol. 6, 2011, pp. 6442 – 6455.

[17] M.A. Quraishi, K.R Ansari, Dileep Kumar Yadav and Eno E. Ebenso, Corrosion Inhibition And Adsorption Studies of Some Barbiturates on Mild Steel/Acid Interface, International Journal of Electrochemical Science, Vol.7, 2012, pp. 12301 – 12315.

[18] P.Udhayakala, T.V. Rajendiran and S. Gunasekaran, Quantum Chemical Studies On The Efficiencies of Vinyl Imidazole Derivatives as Corrosion Inhibitors for Mild Steel, Journal of Advanced Scientific Research, Vol. 3, No. 2, 2012, pp. 37-44.

[19] Gokhan Gece, The Use of Quantum Chemical Methods in Corrosion Inhibitor Studies, Corrosion Science, Vol. 50, No. 11, 2008, pp. 2981–2992, http://dx.doi.org/10.1016/j.corsci.2008.08.043.

[20] K.F. Khaled, Studies Of Iron Corrosion Inhibition using Chemical, Electrochemical and Computer Simulation Techniques, Electrochimica Acta, Vol. 55, No. 22, 2010, pp. 6523–6532, http://dx.doi.org/10.1016/j.electacta.2010.06.027.

[21] I.B.Obot and N.O.Obi-Egbedi, HSAB Descriptors of Thiadiazole Derivatives Calculated by DFT: Possible Relationship as Mild Steel Corrosion Inhibitors, Der Pharma Chemica, Vol. 1, No. 1, 2009, pp. 106-123.

[22] S.Suganthi, V.Kannappan and V.Sathyanarayanamoorthi, Quantum Mechanical Studies on Free Energy of Solution of some Vitamins and their Correlation with Bioavailability, DJ Journal of Engineering Chemistry and Fuel, Vol. 1, No. 1, 2016, pp. 1-14, http://dx.doi.org/10.18831/djchem.org/2016011001

[23] Rawoof Naikoo, Renu Tomar, Muzzaffar Mir, Samiullah Bhat and Radha Tomar, Sorption and Desorption of UO_2^{2+}, Th^{4+}, Eu^{3+}, Ru^{3+} and Fe^{3+} on the Synthetic Analogue of Nepheline, DJ Journal of Engineering Chemistry and Fuel, Vol. 1, No. 1, 2016, pp. 15-16, http://dx.doi.org/10.18831/djchem.org/2016011002

APPENDIX A

Table A1.Inhibition efficiencies of the Schiff bases at various concentrations in 1M H_2SO_4 at 30±1^oC

Concentration, mM	Inhibition Efficiency,% 2hrs immersion		Inhibition Efficiency,% 3hrs immersion		Inhibition Efficiency,% 4hrs immersion		Inhibition Efficiency,% 5hrs immersion		Inhibition Efficiency,% 6hrs immersion	
	SB 1	SB 2	SB 1	SB 2	SB 1	SB 2	SB 1	SB 2	SB 1	SB 2
Blank	-	-	-	-	-	-	-	-	-	-
0.01	18.28	25.43	32.61	38.60	24.33	32.45	18.77	30.76	13.78	28.93
0.05	35.64	58.20	44.07	82.67	29.67	76.53	23.97	70.13	18.47	67.41
0.1	57.10	67.75	69.15	96.98	55.72	80.92	37.68	75.48	25.84	73.24
0.2	62.18	75.48	81.65	97.55	59.46	85.66	44.54	80.33	32.28	78.08
0.3	77.78	83.22	86.69	98.58	73.27	87.56	58.67	82.28	45.60	80.33
0.4	79.38	85.96	88.14	99.30	78.90	89.76	65.77	84.42	54.28	81.26
0.5	80.38	88.23	89.26	99.23	80.33	90.54	70.08	86.76	61.35	84.53
0.6	82.45	88.23	90.58	99.43	84.98	92.75	73.34	88.99	65.35	85.94
0.7	82.45	25.43	90.58	99.43	84.98	92.75	73.34	88.99	65.35	85.94

Table A2.Inhibition efficiency at the maximum concentration of the inhibitors at various temperatures

Name of the inhibitor	Temperature (K)	Inhibition efficiency (%)	Corrosion rate(mpy)
SB 1	303	89.82	15225.82
	313	89.49	16861.66
	323	89.26	31835.82
	333	81.15	34226.65
SB 2	303	99.43	1132.49
	313	98.96	1761.66
	323	98.78	1887.49
	333	98.43	4907.49

Table A3.Effect of addition of 1mM KCl / 1mM KBr / 1mM KI on the inhibition efficiency of the inhibitor

Name of the Inhibitor	Concentration,mM	Inhibition Efficiency,%			
		Without KCl, KBr and KI	With 1mM KCl	With 1mM KBr	With 1mM KI
SB 1	0.02	45.62	61.84	86.93	92.70
	0.04	54.63	71.89	90.25	94.40
	0.06	57.03	80.63	92.22	95.41
	0.08	65.29	84.79	94.97	96.32
	0.1	68.40	86.40	95.19	96.37
SB 2	0.02	81.07	85.44	96.15	97.90
	0.04	90.20	90.47	97.20	98.20
	0.06	94.84	95.45	97.77	98.60
	0.08	96.02	96.76	98.25	98.77
	0.1	96.15	97.42	98.42	99.08

Table A4.Corrosion parameters for mild steel with selected concentrations of the inhibitors in 1M H_2SO_4 by potentiodynamic polarization method

	concentration	Tafel slope Mv/decade		$I_{corr,}$ ($\mu A/cm^2$)	$-E_{corr,}$ mV	Inhibition Efficiency(%)
		b_a	b_c			
	Blank	65	117	287.7	492.1	
SB 1	0.05mM	82	126	242	510.1	15.88
	0.3mM	76	134	167	496.9	41.95
	0.5mM	72	139	29.2	493.5	89.85
SB 2	0.05mM	67	93	34	520.6	88.18
	0.3mM	58	107	33	501.4	88.52
	0.5mM	51	108	12	493.4	95.82

Table A5.Impedance parameters for corrosion of mild steel for selected concentrations of the inhibitors in 1M H_2S0_4

Name of the compound	Concentration(mM)	R_{ct} ohm/ cm^2	$C_{dl}(\mu F)/cm^2$	Inhibition Efficiency(%)
Blank		15.08	28.2	
SB 1	0.05	15.13	30.5	3.30
	0.3	18.37	28.1	17.90
	0.5	24.67	26.2	38.87
SB 2	0.05	16.69	22.1	9.64
	0.3	39.55	14.9	61.87
	0.5	48.61	13.9	68.97

Table A6.Kinetics/Thermodynamic Parameters for mild steel corrosion in 1M H_2SO_4

Name of the inhibitor in mM	Activation energy, E_a (KJ/mole)	$-\Delta G^0_{ads}$(KJ/mole)				$-\Delta H^0$ KJ/mole	$-\Delta S^0$ KJ/mole
		303 K	313 K	323K	333 K		
Blank	37.3265	-	-	-	-	-	-
SB 1	39.60	17.20	17.76	18.33	18.90	25.6858	0.9983
SB 2	41.48	14.87	15.69	16.51	17.33	65.6555	1.9705

Table A7. Table S1 Quantum chemical parameters for SB 1 and SB 2

Parameters	SB 1	SB 2
E_{HOMO}	-6.719088272	-6.025192472
E_{LUMO}	-2.51979416	-2.096381664
Energy gap, ΔE /eV	4.199294112	3.928810808
Ionisation potential, I /eV	6.719088272	6.02519
Electron affinity, A /eV	2.51979416	2.09638
Dipole moment in Debye	5.0585	4.6194
Transferred electrons fractions, ΔN	0.56689499	0.748111839
Global Softness, S	0.47627052	0.50906
Global Hardness, η	2.09964706	1.964405
Electronegativity, χ	4.61944122	4.060785
Chemical potential, μ	-4.61944122	-4.060785
Electrophilicity, ω	5.08162481	4.19719325
Total energy, TE, (a.u)	-817.74899386	-1140.67792368

Table A8.Fukui and local softness indices for nucleophilic and electrophilic attacks in SB 1 atoms calculated from Mulliken atomic charge

Atom number	qN+1	qN-1	qN	f^+_k	f^-_k	s_k+	s_k-
H1	0.122657	0.042454	0.129765	-0.007108	0.087311	-0.0033853	0.04158366
C2	-0.111673	-0.162703	-0.311912	0.200239	-0.149209	0.09536793	-0.0710638
C3	-0.087082	-0.09253	0.094189	-0.181271	0.186719	-0.086334	0.08892876
C4	-0.072688	-0.115806	-0.170406	0.097718	-0.0546	0.0465402	-0.0260044
C5	-0.083775	-0.107752	-0.281312	0.197537	-0.17356	0.09408105	-0.0826615
C6	0.251467	0.215726	-1.238197	1.489664	-1.453923	0.70948305	-0.6924607
C7	0.108041	0.145202	1.19665	-1.088609	1.051448	-0.5184724	0.50077369
C8	-0.107163	-0.213938	-0.240428	0.133265	-0.02649	0.06347019	-0.0126164
C9	0.056161	0.103545	0.034064	0.022097	-0.069481	0.01052415	-0.0330918
C10	0.526466	0.458308	0.382468	0.143998	-0.07584	0.068582	-0.0361204
N11	-0.57554	-0.64283	-0.366	-0.20954	0.27683	-0.0997977	0.13184597
H12	0.133139	0.03718	0.131813	0.001326	0.094633	0.00063153	0.04507091
H13	0.137198	0.035119	0.132879	0.004319	0.09776	0.00205701	0.04656021
H14	0.134413	0.047043	0.13749	-0.003077	0.090447	-0.0014655	0.04307724
H15	0.136577	0.04229	0.1372	-0.000623	0.09491	-0.0002967	0.04520284
O16	-0.529304	-0.509011	-0.407859	-0.121445	0.101152	-0.0578407	0.04817572
H17	0.351865	0.292874	0.388733	-0.036868	0.095859	-0.0175591	0.04565482
C18	0.105874	0.039873	0.188889	-0.083015	0.149016	-0.0395376	0.07097193
H19	0.196276	0.032412	0.108066	0.08821	0.075654	0.04201182	0.03603177
N20	-0.340703	-0.541168	-0.052909	-0.287794	0.488259	-0.1370678	0.23254337
C21	0.291382	0.294971	-0.825154	1.116536	-1.120125	0.53177318	-0.5334825
C22	-0.055938	-0.126666	0.387482	-0.44342	0.514148	-0.2111879	0.24487354
C23	0.105067	0.065869	-0.329659	0.434726	-0.395528	0.20704718	-0.1883783
N24	-0.371993	-0.487979	-0.186653	-0.18534	0.301326	-0.088272	0.14351269
C25	0.105394	0.071768	-0.250759	0.356153	-0.322527	0.16962517	-0.1536101
C26	-0.057252	-0.122146	0.698924	-0.756176	0.82107	-0.3601443	0.39105144
H27	0.153479	0.054051	0.12329	0.030189	0.069239	0.01437813	0.03297649
H28	0.16169	0.0445	0.126485	0.035205	0.081985	0.0167671	0.03904704
H29	0.161736	0.043507	0.127862	0.033874	0.084355	0.01613319	0.0401758
H30	0.15423	0.055837	0.134998	0.019232	0.079161	0.00915963	0.03770205

Table A9.Fukui and local softness indices for nucleophilic and electrophilic attacks in SB 2 atoms calculated from Mulliken atomic charge

Atom number	qN+1	qN-1	qN	f^+_k	f^-_k	s_k+	s_k-
H1	0.134223	0.045357	0.090758	0.043465	0.045401	0.022126	0.023112
C2	-0.116384	-0.159325	-0.128114	0.01173	0.031211	0.005971	0.015888
C3	-0.073567	-0.09103	-0.093204	0.019637	-0.002174	0.009996	-0.00111
C4	-0.075825	-0.115821	-0.08955	0.013725	0.026271	0.006987	0.013374
C5	-0.063951	-0.096299	-0.079618	0.015667	0.016681	0.007975	0.008492
C6	0.248352	0.205091	0.231226	0.017126	0.026135	0.008718	0.013304
C7	0.124141	0.145569	0.119997	0.004144	-0.025572	0.00211	-0.01302
C8	-0.099057	-0.192939	-0.1308	0.031743	0.062139	0.016159	0.031632
C9	0.076266	0.10249	0.081696	-0.00543	-0.020794	-0.00276	-0.01059
C10	0.054186	0.05144	0.059819	-0.005633	0.008379	-0.00287	0.004265
N11	-0.506516	-0.562193	-0.537653	0.031137	0.02454	0.015851	0.012492
H12	0.146721	0.041188	0.093312	0.053409	0.052124	0.027188	0.026534
H13	0.146749	0.03931	0.09551	0.051239	0.0562	0.026084	0.028609
H14	0.145236	0.055176	0.103114	0.042122	0.047938	0.021443	0.024403
H15	0.142547	0.043399	0.098941	0.043606	0.055542	0.022198	0.028274
S16	0.263299	0.015092	0.089786	0.173513	0.074694	0.088329	0.038024
H17	0.121441	0.022513	0.058779	0.062662	0.036266	0.031899	0.018462
C18	0.150352	0.065357	0.130618	0.019734	0.065261	0.010046	0.033222
H19	0.157362	0.039359	0.086733	0.070629	0.047374	0.035954	0.024116
N20	-0.455684	-0.565451	-0.439432	-0.016252	0.126019	-0.00827	0.064151
C21	0.262015	0.294579	-0.06231	**0.324325**	-0.356889	**0.165101**	-0.18168
C22	-0.083228	-0.125831	-0.093429	0.010201	0.032402	0.005193	0.016495
C23	0.100902	0.065685	0.383365	-0.282463	**0.31768**	-0.14379	**0.161718**
N24	-0.385322	-0.486261	-0.451615	0.066293	0.034646	0.033747	0.017637
C25	0.104108	0.071775	0.094862	0.009246	0.023087	0.004707	0.011753
C26	-0.081036	-0.1214	-0.098618	0.017582	0.022782	0.00895	0.011597
H27	0.125374	0.053855	0.099324	0.02605	0.045469	0.013261	0.023146
H28	0.147933	0.046114	0.093054	0.054879	0.04694	0.027937	0.023895
H29	0.148936	0.046447	0.100723	0.048213	0.054276	0.024543	0.02763
H30	0.140425	0.066754	0.092728	0.047697	0.025974	0.024281	0.013222

Table A10.Fukui function and local softness average for four atoms (three Nitrogen atoms and one Oxygen atom for SB 1 and three Nitrogen atoms and one Sulphur atom for SB 2)

Average values	SB 1	SB 2
f_k^+	-0.2019	+0.0636
f_k^-	+0.2918	+0.0649
s_k+	-0.09574	+0.03241
s_k-	+0.1389	+0.03307

APPENDIX B

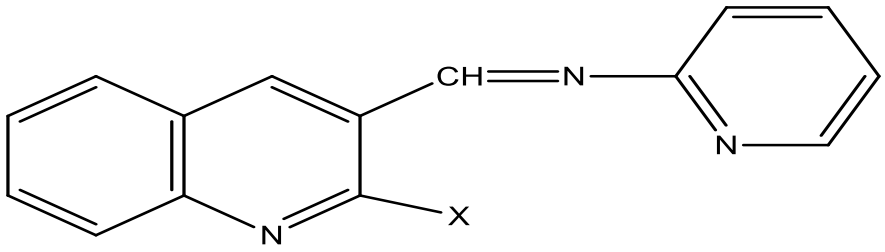

X=OH.....(SB 1)
X=SH.....(SB 2)

3-((pyridin-2-ylimino)methyl)quinoline-2-ol/thiol

Figure B1.Schematic structure of Schiff base

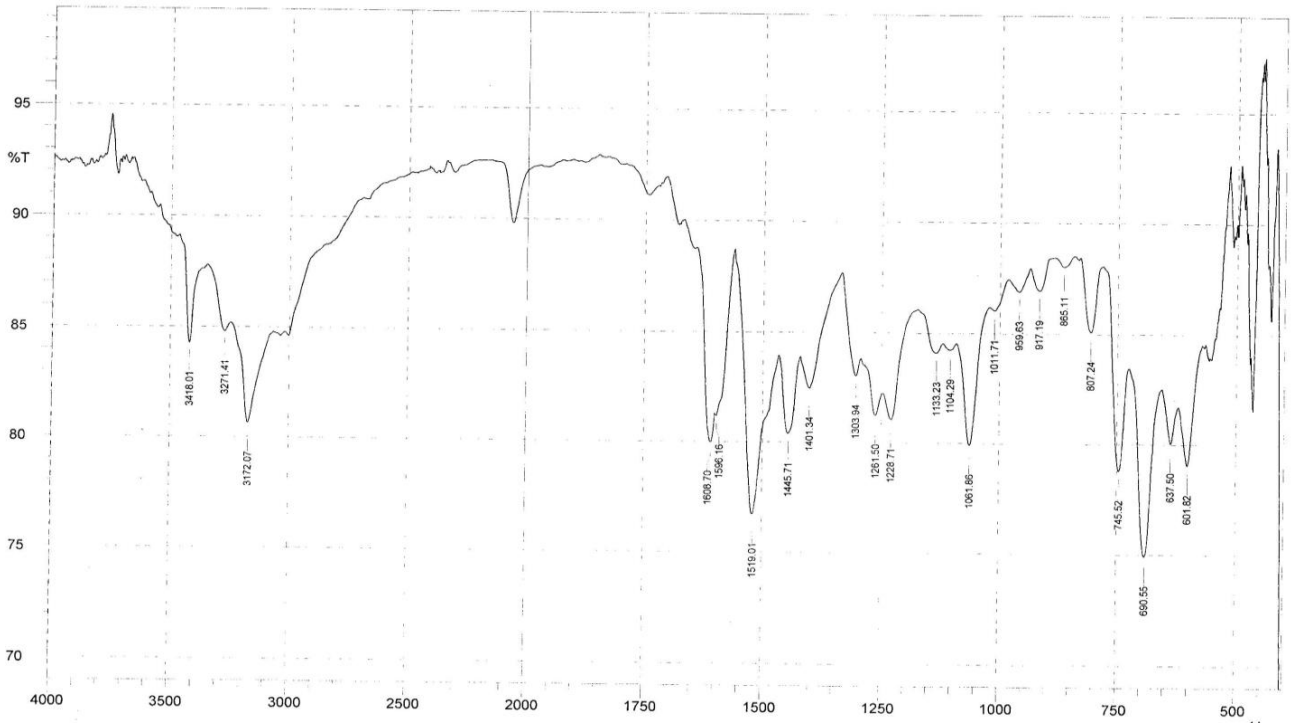

Figure B2.FTIR spectra for the compound SB 1

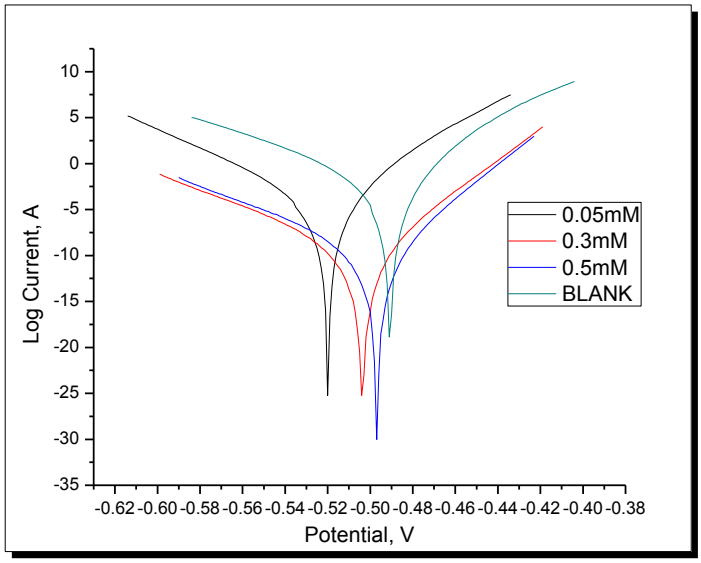

Figure B3.Tafel lot for the inhibitor SB 2

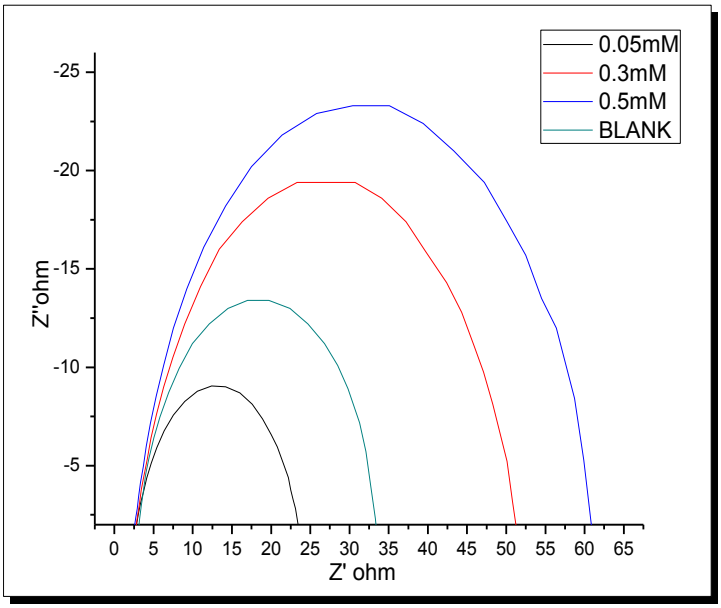

Figure B4.Nyquist plot for the inhibitor SB 2

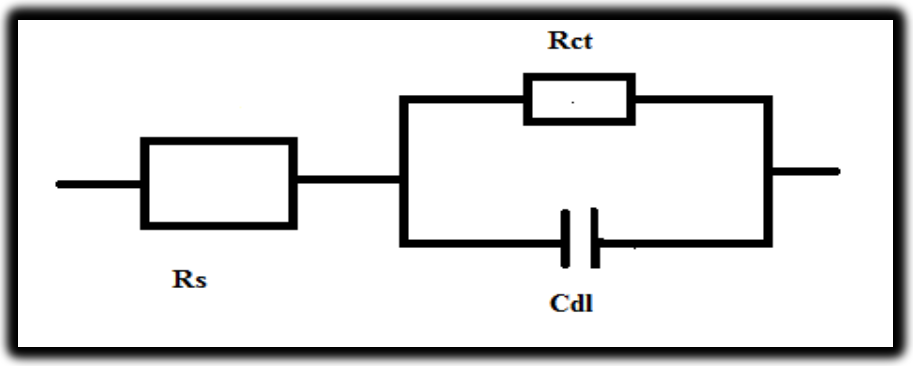

Figure B5.Electrochemical equivalent circuit impedance spectra.

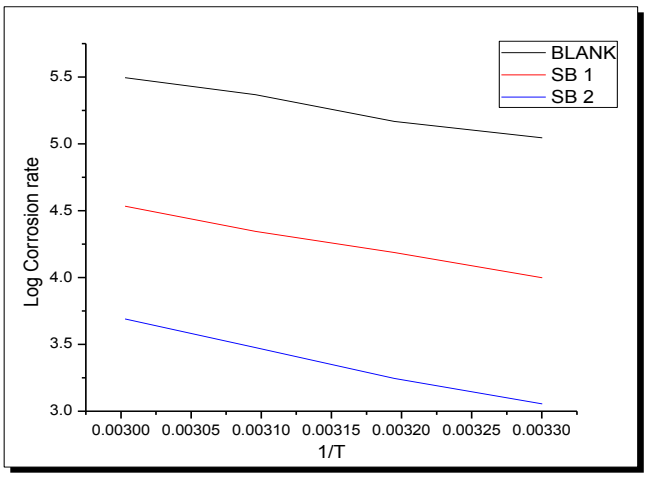

Figure B6.Arrhenius plot

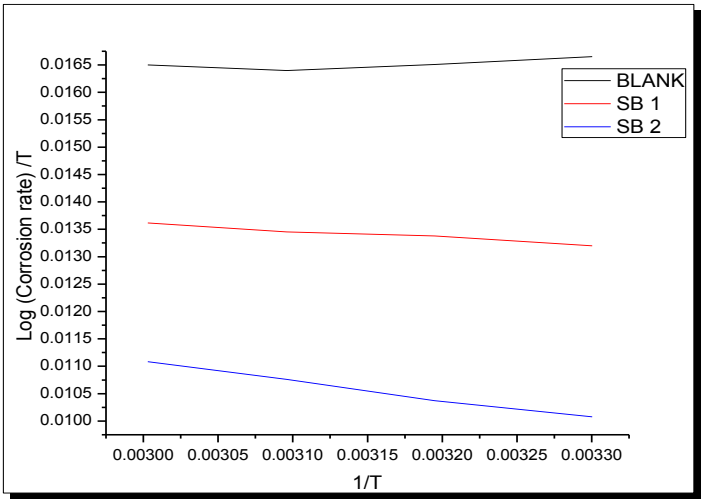

Figure B7.Transition state plot

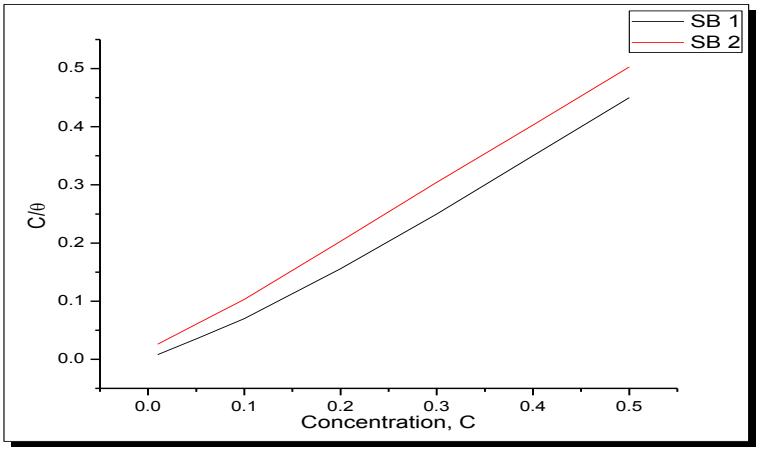

Figure B8.Langmuir adsorption isotherm

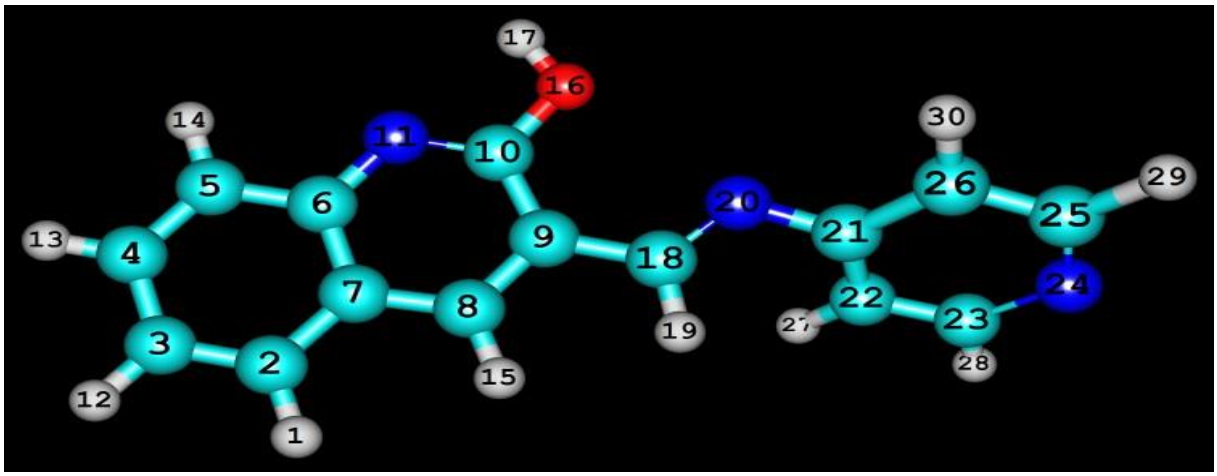

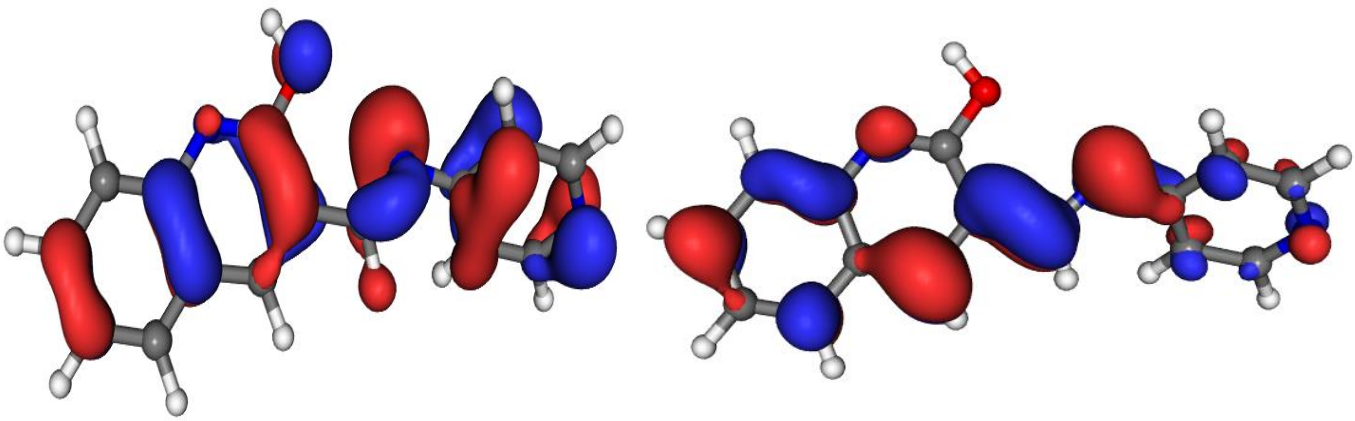

Figure B9.Optimised and HOMO, LUMO geometry of SB 1

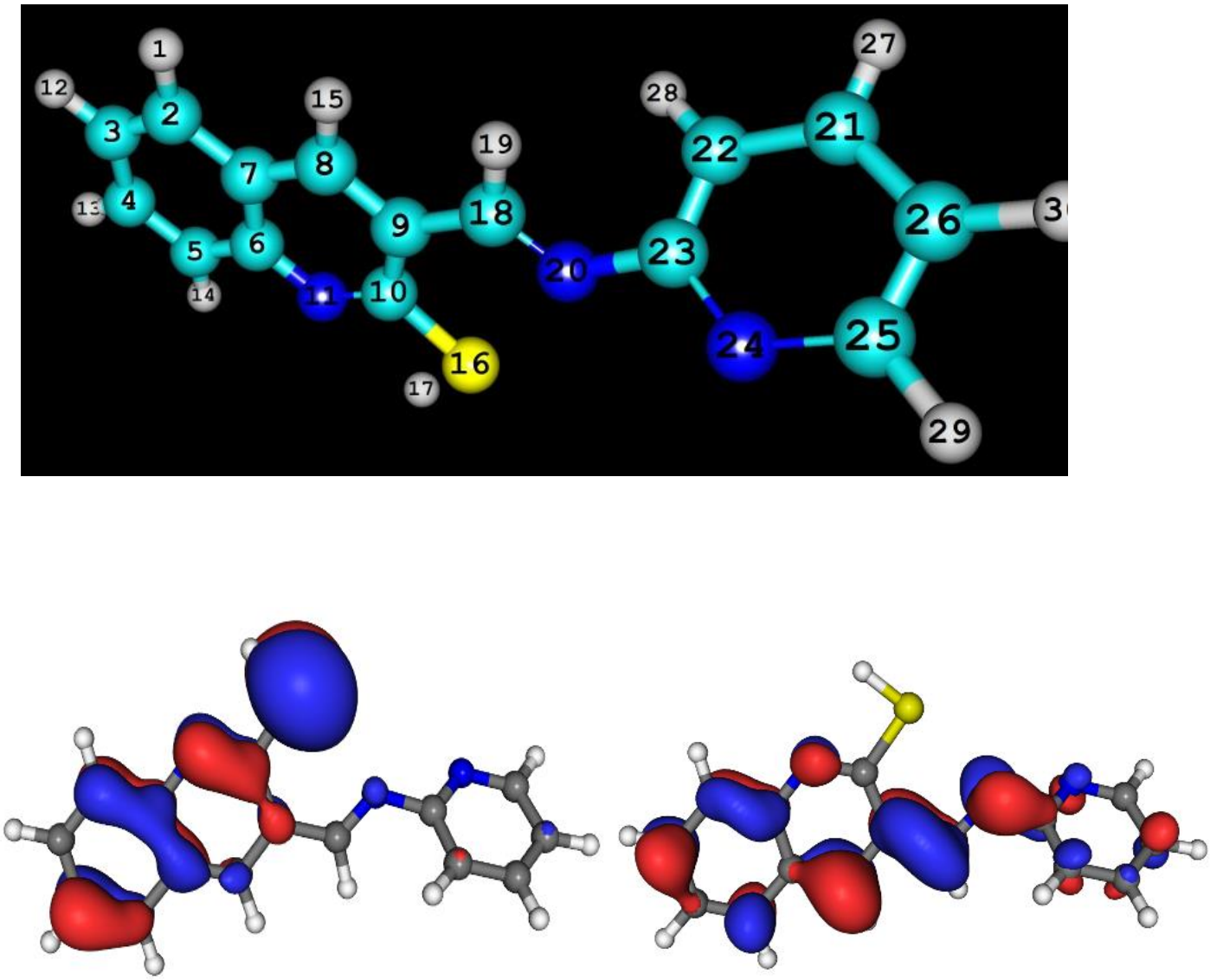

Figure B10.Optimised and HOMO, LUMO geometry of SB 2